

## ELECTROSPRAYING OF ZnO MICROSTRUCTURES FOR ELECTRICAL CONTACTING

A. COSTAS, C. FLORICA\*, A. EVANGHELIDIS, M. ENCULESCU,  
N. PREDA, I. ENCULESCU

*National Institute of Materials Physics, Magurele, Bucharest, P.O. Box MG-7,  
077125, Romania*

ZnO complex microstructures were deposited onto interdigitated metallic electrodes by electrospaying. Simple methods, such as wet chemical precipitation and optical lithography, were used for the synthesis of flower-like and snowflake-like ZnO structures and for the preparation of interdigitated metallic electrodes, respectively. The electrospayed ZnO particles preserve the structural, optical and morphological properties of the chemically synthesized ZnO powders. During the electrospaying process, the ZnO microstructures form bridges between the interdigitated metallic electrodes leading to electrical contacting. Changes in the electron transport through the ZnO microstructures are evidenced by their exposure to ammonia or their passivation with poly(methyl methacrylate). Merging such easy-scalable and low-cost techniques, devices based on electrospayed complex ZnO structures can be designed.

(Received July 13, 2015; Accepted October 19, 2015)

*Keywords:* ZnO microstructures; interdigitated metallic electrodes;  
Electrospaying; ammonia; PMMA passivation

### 1. Introduction

During the last decade, electrospaying has emerged as a powerful and suitable technique in micro/nanotechnologies as a solution for the preparation of functional metal oxide micro/nanostructures [1-5]. The main benefits of this method are the simplicity and the cost-effectiveness of the setup, which operates at ambient atmosphere with high deposition efficiency. Recently, due to the ZnO's unique properties (direct band gap (3.37 eV at 300 K), relatively large exciton binding energy (60 meV), high mechanical, thermal and chemical stability, etc.) [6], a particular interest was given to the electrospaying of ZnO particles [7, 8]. The semiconducting structures can be directly electrospayed from their dispersions [7] or can be synthesized during or after the electrospaying process by using zinc salts solutions as precursors for ZnO preparation [8]. Furthermore, features such as its rich family of structure morphologies (wires, rods, prisms, tubes, etc.), high occurrence, non-toxicity and low-price recommend ZnO structures for integration in relatively low-cost electronic and optoelectronic devices [9-12]. Generally, when such devices are designed, a patterning technique for producing metallic electrodes, like photolithography (highly efficient and low-cost technique, yielding large patterned surfaces in a short time using only UV light) is combined with a ZnO preparation method in order to achieve functionality.

In this context, chemically synthesized ZnO powders containing complex microstructures (flowers and snowflakes) were electrospayed on photolithographically prepared interdigitated metallic electrodes. The structural, optical, morphological and electrical properties of the electrospayed ZnO microstructures were studied using X-ray diffraction, reflectance, photoluminescence, scanning electron microscopy and current-voltage measurements. Usually, in order to investigate the electrical properties of the ZnO structures, these are covered by conducting layers used as electrodes [13, 14]. As an alternative, by electrospaying the ZnO microstructures onto the interdigits, their electrical properties can be evaluated without any additional contacting

---

\* Corresponding author: camelia.florica@infim.ro

steps, taking into account that the electrodes are connected by junctions formed directly by the semiconducting particles providing electrical paths. To emphasize changes in the electron transport through the electrospayed ZnO microstructures, the electrical measurements were carried out while exposing the samples to ammonia vapors or after covering them with a thin layer of poly(methyl methacrylate). This kind of information is helpful for designing devices based on such electrospayed semiconducting structures.

## 2. Experimental

ZnO powders with different morphologies were prepared by wet chemical precipitation according to the procedure presented in Ref. [15], using as reactants zinc nitrate ( $\text{Zn}(\text{NO}_3)_2$ ) and an alkaline compound such as sodium hydroxide (NaOH) or potassium hydroxide (KOH). Depending on the precipitating agent, ZnO particles having flower-like structures (NaOH) or snowflake-like structures (KOH) were obtained, the mechanism responsible for the formation of these two morphologies being described in Ref. [16, 17]. All chemicals were purchased from Sigma-Aldrich. Briefly, a 0.01 M  $\text{Zn}(\text{NO}_3)_2$  aqueous solution was placed in a thermostatic bath under continuous stirring and when it reached 90 °C a 0.01 M alkaline aqueous solution (NaOH or KOH) was added. After 3 h the synthesized ZnO white powder was collected through centrifugation, washed several times with distilled water and dried on filter paper at room temperature. By ultrasonicing the synthesized ZnO powder in ethanol for 15 min, a homogeneous suspension (5 wt %) was obtained to be further used in the electrospaying process. The ZnO particles suspension was introduced in a syringe pump (New Era Pump System).

In order to use a specific metallic collector in the electrospaying technique, interdigitated metallic electrodes (IME) were prepared on  $\text{SiO}_2/\text{Si}$  wafer by standard photolithography in a cleanroom class 100 (ISO EN 14644). Thus, a photoresist (AZ5214E - Microchemicals) was spin-coated on the  $\text{SiO}_2/\text{Si}$  substrate and, by UV light exposures and thermal treatments through a mask, the IME were formed on a 0.4 mm<sup>2</sup> size area having widths of 4 μm and gaps of 4 μm. After the developing procedure, the deposition of the Ti/Au thin layer was made in a TECTRA equipment using RF sputtering (10 nm Ti layer) and thermal vacuum evaporation (90 nm Au layer). The Ti layer is required for the improvement of the adhesion of the Au layer to the  $\text{SiO}_2/\text{Si}$  substrate. After removing the photoresist in acetone, the interdigitated Ti/Au electrodes can be used as metal collectors for the deposition of ZnO particles by electrospaying. The syringe pump containing the ZnO particles suspension was connected through the metallic needle to a high voltage power supply (30kV Spellman SL300). The electrospaying process parameters were: 10 ml/h solution flow rate, 20 kV applied voltage and 20 cm needle-to-metal collector distance. The electrospayed particles deposited on IME were dried under ambient atmosphere, a simplified illustration of the process being presented in Fig. 1.

As it can be seen in the optical photographs and the scanning electron microscopy (SEM) images (Fig. 2), for both types of ZnO morphology (flower or snowflake), the electrospaying results in completely covered substrates containing the interdigitated metallic electrodes.

The structural, optical and morphological properties of the electrospayed ZnO particles were investigated using X-ray diffraction, reflectance, photoluminescence and scanning electron microscopy. For the X-ray diffraction characterization, a Bruker AXS D8 Advance instrument with Cu K $\alpha$  radiation ( $\lambda = 0.154$  nm) was used. The source was operated at 40 kV and 40 mA and the K $\alpha$  radiation was removed using a nickel filter. The total reflection spectra were measured using a Perkin-Elmer Lambda 45 UV-VIS spectrophotometer equipped with an integrating sphere. The photoluminescence measurements were performed at 350 nm excitation wavelength using FL 920 Edinburgh Instruments spectrometer with a 450 W Xe lamp excitation and double monochromators on both excitation and emission. The morphologies of the samples were evaluated using a Zeiss Evo 50 XVP scanning electron microscope. Also, the electrical properties of the electrospayed ZnO particles were characterized using a Keithley 4200 SCS and a Cascade Microtech MPS 150 probe station. The current–voltage characteristics were obtained by a conventional two-probe method for the samples in air, when exposed to ammonia vapors and when covered with a thin layer of poly(methyl methacrylate) (PMMA). The PMMA layer was obtained

by spin-coating at 6000 rpm for 30s a commercially available solution of PMMA 7% in anisole (Microchemicals).

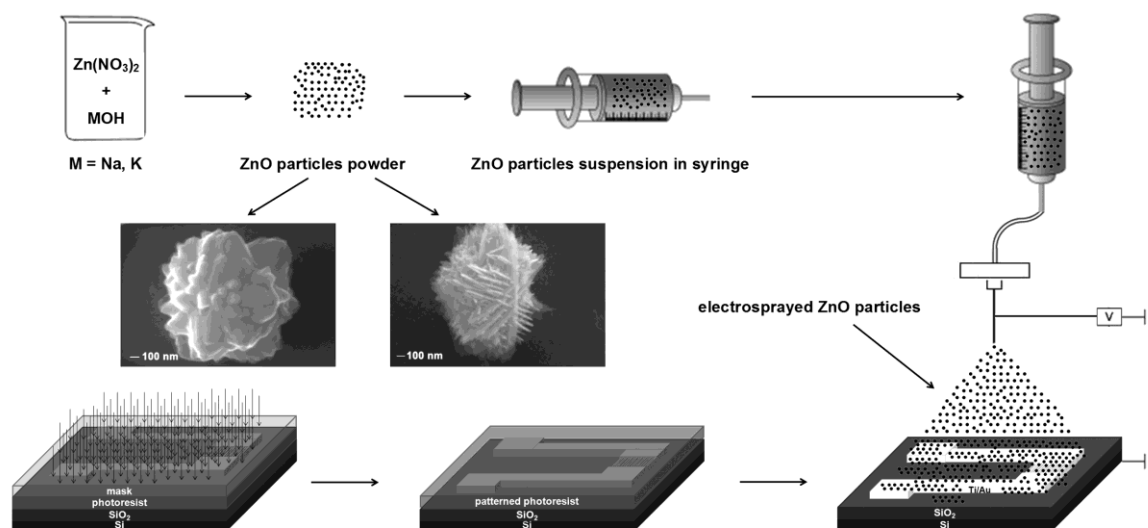


Fig. 1. Schematic representation of the experimental procedures involved in the electrospinning of ZnO microstructures on interdigitated metallic electrodes

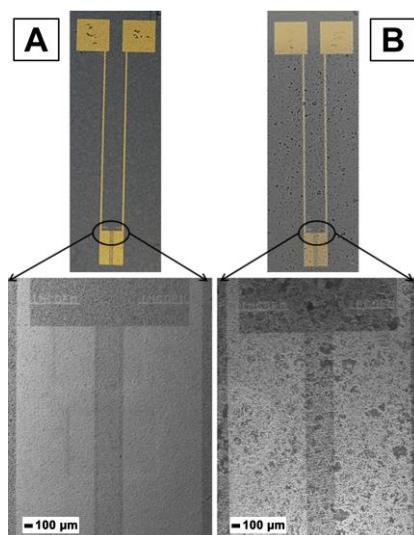


Figure 2. Optical photographs and SEM images of SiO<sub>2</sub>/Si containing interdigitated metallic electrodes covered by electrospun ZnO microstructures chemically synthesized from  $Zn(NO_3)_2$  and NaOH (A) or KOH (B).

### 3. Results and discussion

In order to confirm that the electrospinning process did not affect the properties of the ZnO particles in powder form, the structural, optical and morphological properties of the electrospun ZnO particles deposited on IME were investigated. Thus, the X-ray diffraction patterns presented in Fig. 3A show four peaks corresponding to the Miller indexes of the reflecting planes for ZnO (100), (002), (101) and (102) (JCPDS file no. 36-1451) proving the formation of ZnO hexagonal wurtzite phase and other three peaks which characteristic to the substrate (Si and Au). The room temperature reflectance and photoluminescence spectra of the electrospun ZnO particles deposited on IME are shown in Fig. 3B and Fig. 3C, respectively.

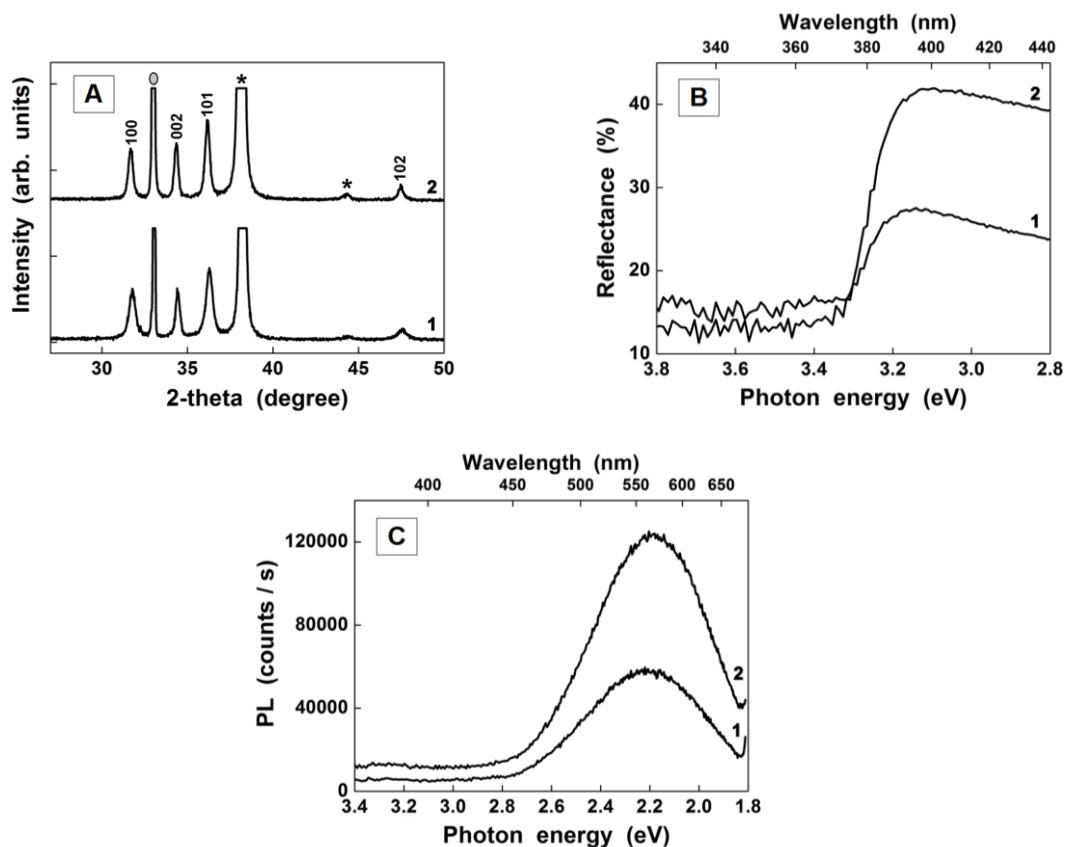


Fig. 3. X-ray diffraction patterns (A), Reflectance spectra (B) and Photoluminescence spectra (C) of electrospayed ZnO microstructures chemically synthesized from  $\text{Zn}(\text{NO}_3)_2$  and NaOH (curve 1) or KOH (curve 2). Peaks attributed to Si ( $\circ$ ) and Au ( $*$ ).

Analyzing the reflectance data, a strong decrease can be noticed below 380 nm, this being attributed to the ZnO band-to-band transition. In both cases, the band gap value was estimated at around 3.25 eV by using the Kubelka–Munk function  $F(R) = (1-R)^{1/2} / 2R$ , where R is the observed diffuse reflectance. Regarding the emission data, the photoluminescence spectra exhibit only a strong, broad emission band centered at about 560 nm ( $\sim 2.2$  eV) linked to the incorporation of hydroxyl groups in the crystal lattice during the growth process and to the oxygen defects (interstitial ions or vacancies) [18, 19]. Typically, the ZnO emission spectra display two main emission bands: one in UV domain, of excitonic origin, and another, in the visible range, linked to defects [20]. In our case, the absence of the excitonic emission in the samples photoluminescence spectra can be explained by taking into account the preparation method of the ZnO particles. Thus, in the wet chemical synthesis methods, the ZnO crystallites are formed by  $\text{Zn}(\text{OH})_2$  dehydration, traces of this compound on the ZnO surface can lead to the quenching of the ZnO exciton emission [21]. Therefore, the structural and optical properties of electrospayed ZnO microstructures preserve the properties of the ZnO particles synthesized as powders [15].

In order to find whether the ZnO particles morphology is affected by the electrospaying process or not, the samples were investigated by SEM (Fig. 4). In both cases, the low magnification SEM images (Fig. 4A and Fig. 4C) reveal that the electrospayed ZnO particles cover both the IME and the gaps between them. As it is shown in the high magnification SEM images (Fig. 4B and Fig. 4D), after the electrospaying process, the ZnO particles have the same morphologies as those observed in the case where they are in powder form [15] having the flower and snowflake like shapes, formed by assembled leaves (Fig. 4B) and platelets (Fig. 4D), respectively and having sizes in the 1-2  $\mu\text{m}$  range.

In the case of the ZnO microstructures electrospayed on IME, the main advantage is given by the formation of ZnO bridges onto the IME as it can be observed in Fig. 5, providing in

this way electrical paths between the neighboring grid structures. Taking into account that ZnO structures based devices are sensitive to surface-adsorbed oxygen and/or water molecules, which influence their electrical properties [22, 23], the current-voltage measurements were carried out when exposing the ZnO samples to ammonia vapors (Fig. 6A and Fig. 6C) and when they were covered with a PMMA thin layer (Fig. 7A and Fig. 7C).

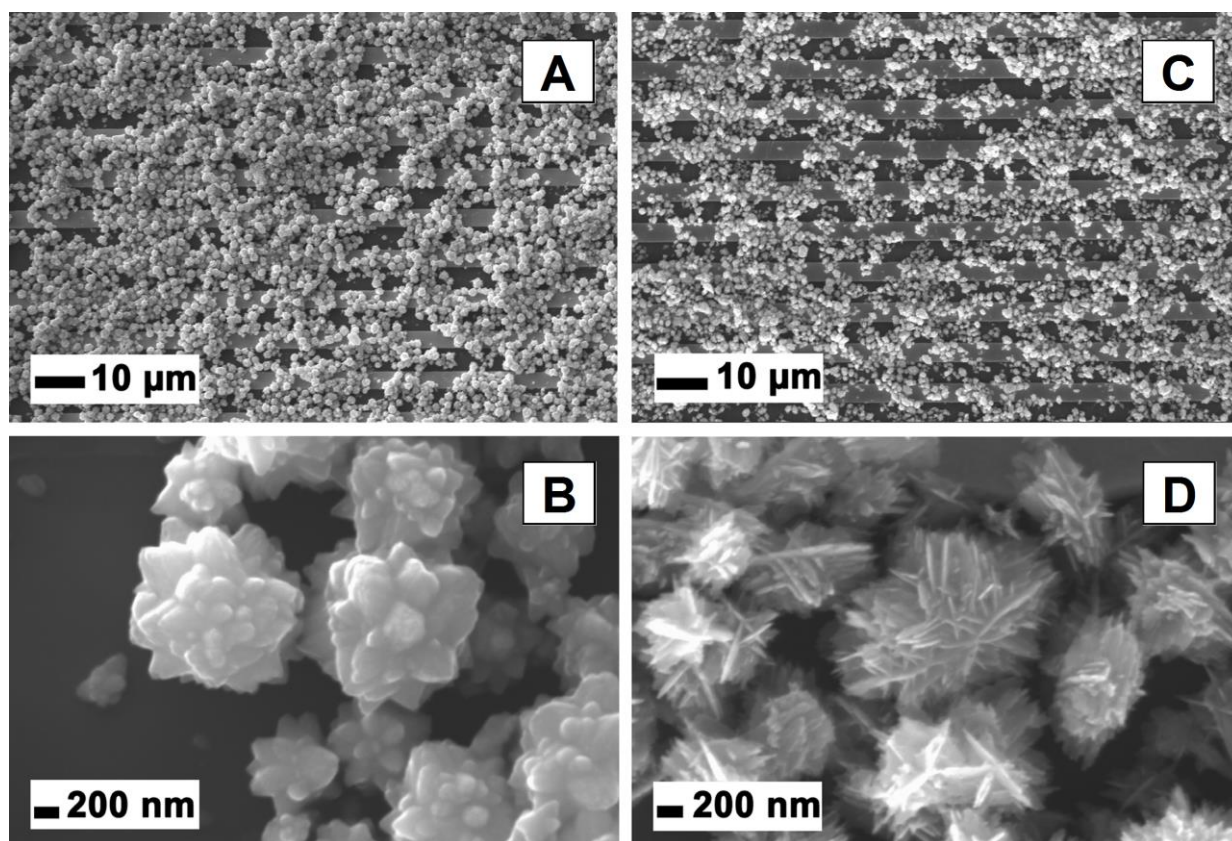


Fig. 4. SEM images (at different magnifications) of electrospayed ZnO microstructures on interdigitated metallic electrodes: flowers (A, B) and snowflakes (C, D).

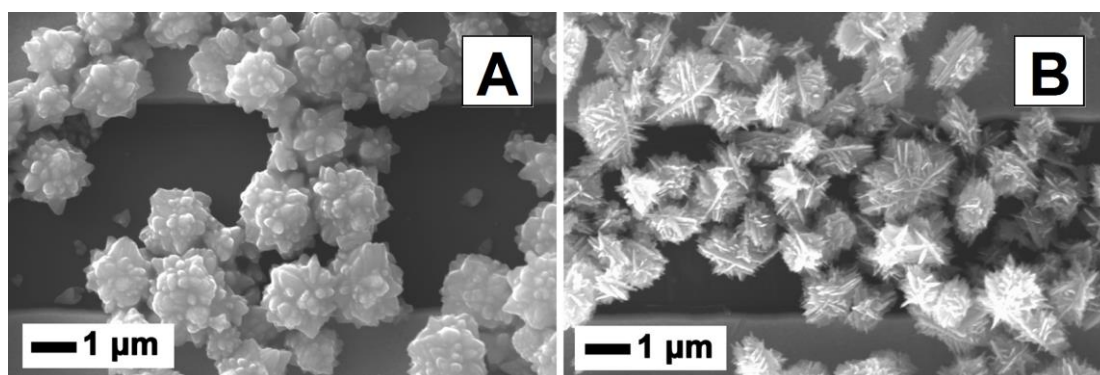


Fig. 5. SEM images of bridges formed by electrospayed ZnO microstructures on interdigitated metallic electrodes: flowers (A) and snowflakes (B)

Regardless of their morphology, the transport of charges takes place by percolating through the formed junctions over the interdigits, travelling from one ZnO microstructure to another until reaching the metallic electrodes (Fig. 5A and Fig. 5B), and depends on the concentration of free electrons in the conduction band. Any modification that could occur at the



surface of the ZnO microstructures can induce a change in the electrical characteristics. The adsorbed oxygen can extract electrons available for conduction and become  $O_2^-$ ,  $O^-$ , or  $O^{2-}$  species [24]. As shown in Fig. 6A and Fig. 6C a decrease in current takes place when exposing to ammonia either flower or snowflake like microstructures. The resistance increases after the samples' exposure to ammonia are presented in the Fig. 6B and Fig. 6D. The adsorption of oxygen or water molecules can be enhanced by the presence of ammonia, leading to an increase in resistance up to a saturation point reached when the adsorption processes are also saturated [22, 25].

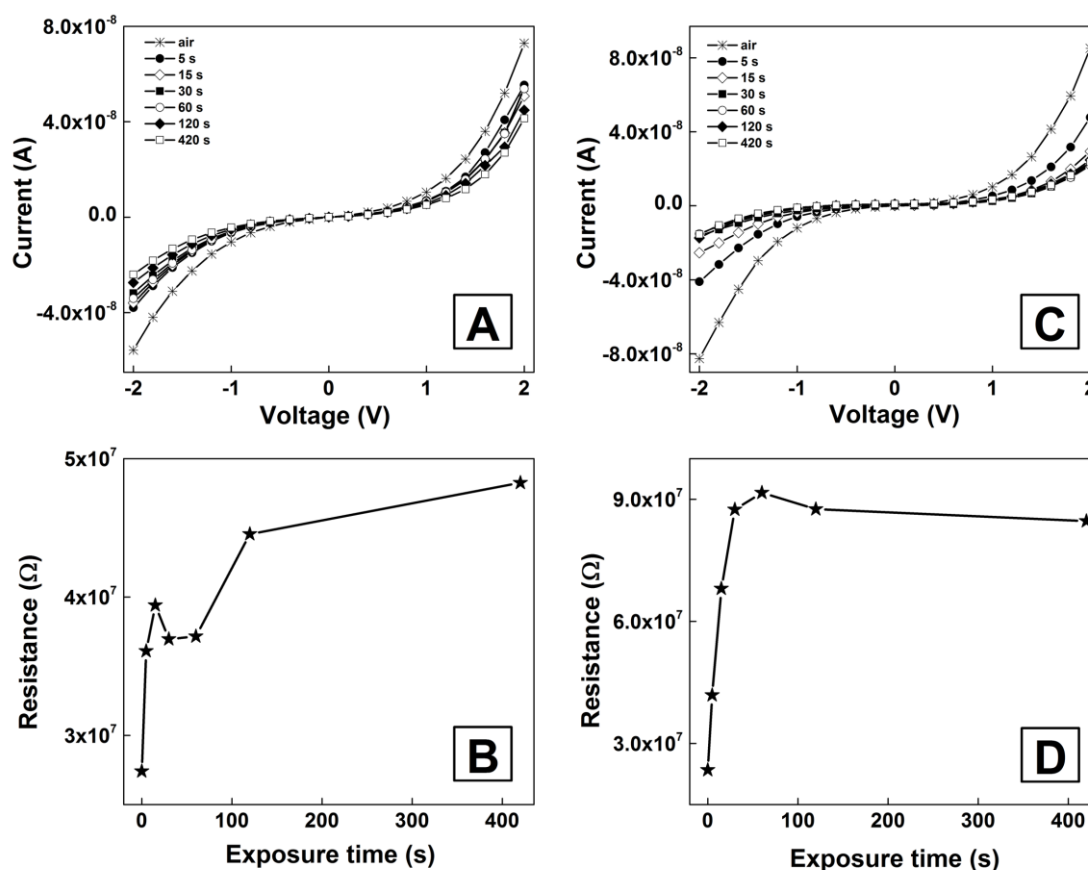


Fig. 6. Changes induced in the current–voltage characteristics of electrospayed ZnO microstructures on interdigitated metallic electrodes by their exposure to ammonia (A, C) and the resistance variation of the ZnO samples (at 2 V) with the time of exposure to ammonia (B, D): flowers (A, B) and snowflakes (C, D).

Instead, if the surface of the ZnO microstructures is covered by a layer, this can provide insulation between the surface and the ambient environment, resulting in no interaction between the adsorbed ions and the electrons from the conduction band. Thus, the surface passivation with a PMMA layer is bound to lead to an increase in current and therefore a lower resistance [26], as shown in Fig. 7A and Fig. 7C. Furthermore, a gradual increase in current can be noticed with the PMMA solvent's (anisole) evaporation time, up to a saturation current given by the formation of a compact polymer film.

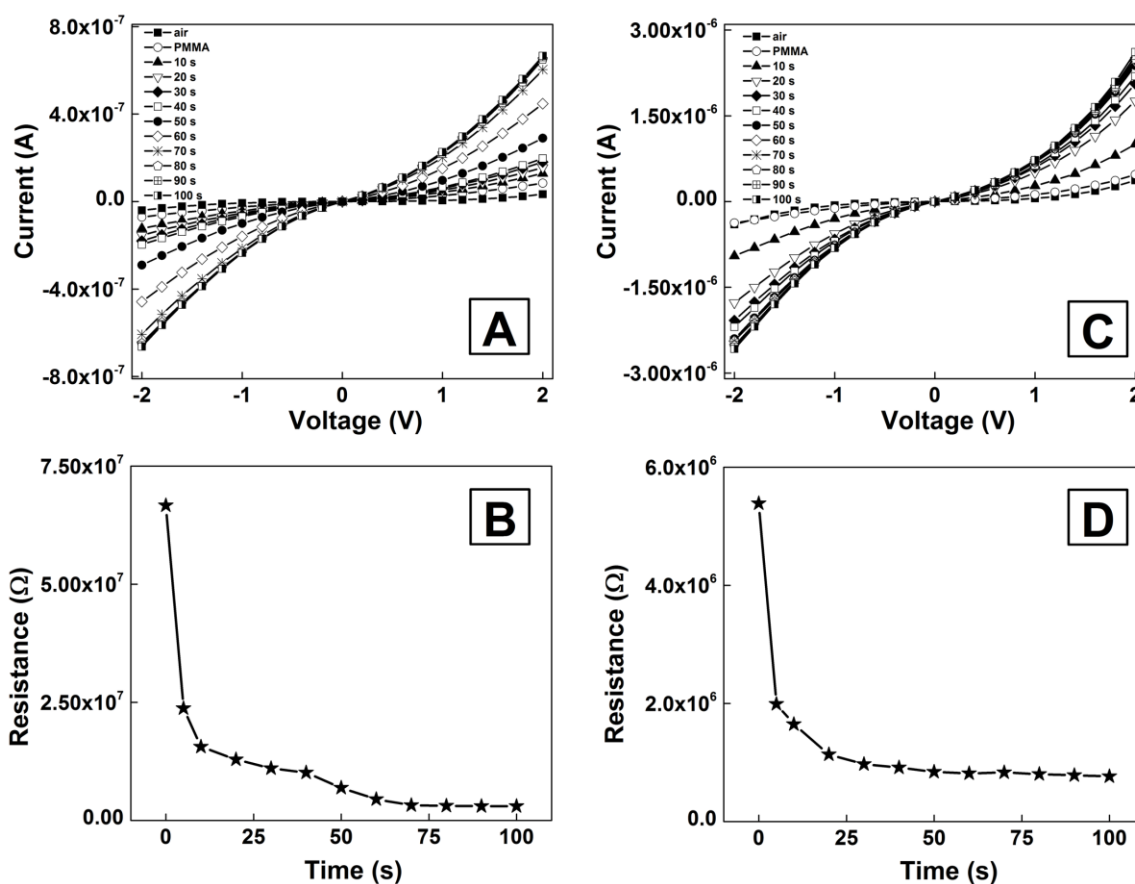


Fig. 7. Changes induced in the current–voltage characteristics of electrosprayed ZnO microstructures on interdigitated metallic electrodes by their passivation with PMMA (A, C) and the resistance variation of the ZnO samples (at 2 V) with the PMMA's solvent evaporation time (B, D): flowers (A, B) and snowflakes (C, D).

In the same time, a decrease in the samples' resistance is observed in the insets of Fig. 7B and Fig. 7D. The ZnO microstructures are sensitive to the anisole vapors that are present on their surface inducing changes in the current-voltage characteristics in the rather short time of the PMMA solvent evaporation. The saturation of the current, and of course of the resistance, takes place when the evaporation process is over and the ZnO microstructures surfaces are insulated from the ambient environment.

#### 4. Conclusions

The electrospraying of ZnO microstructures on interdigitated metallic electrodes leads to the formation of ZnO bridges between the interdigits, providing electrical paths. After the electrospraying process, the ZnO microstructures have the same structural (hexagonal wurtzite), optical (band-gap and emission band) and morphological (flowers and snowflakes shapes) properties as those observed when they are in powder form. The electrical measurements revealed that the electrosprayed ZnO microstructures are sensitive to any adsorption processes taking place at their surfaces when they are exposed to ammonia vapors, or when they are covered with a thin layer of PMMA. Therefore, electrospraying of ZnO microstructures is an effective technique for fabricating devices with potential applications in electronic and optoelectronic devices (sensors, transistors, etc.). Also, the results described herein are of great interest taking into account that the methods used in samples preparation, wet chemical precipitation, conventional photolithography

and electrospaying, are low-cost and easily scalable, being efficient and suitable for industrial processing.

### Acknowledgements

This work was supported by a grant of the Romanian National Authority for Scientific Research, CNCS – UEFISCDI, project number PN-II-RU-TE-2012-3-0148 and by the Contract 45 N, Project PN09-450102. Andreea Costas was supported by the strategic grant POSDRU/159/1.5/S/137750, "Project Doctoral and Postdoctoral programs support for increased competitiveness in Exact Sciences research" cofinanced by the European Social Found within the Sectorial Operational Program Human Resources Development 2007 – 2013.

### References

- [1] J. Xie, J. Jiang, P. Davoodi, M. P. Srinivasan, C.-H. Wang, *Chem. Eng. Sci.*, **125**, 32 (2015)
- [2] A. Jaworek, A.T. Sobczyk, *J. Electrostat.*, **66**, 197 (2008)
- [3] O. V. Salata, *Curr. Nanosci.*, **1**, 25 (2005)
- [4] O. Kilo, J. Jabbour, R. Habchi, N. Abboud, M. Brouche, A. Khoury, D. Zaouk, *Mater. Sci. Semicond. Process.*, **24**, 57 (2014)
- [5] C. M. Ghimbeu, M. Lumbreras, J. Schoonman, M. Siadat, *Sensors*, **9**, 9122 (2009)
- [6] A. Janotti, C. G. Van de Walle, *Rep. Prog. Phys.*, **72**, 126501 (2009)
- [7] K. H. Choi, S. Khan, H. W. Dang, Y. H. Doh, S. J. Hong, *Jpn. J. Appl. Phys.*, **49**, 05EC08 (2010)
- [8] C. T. Pan, Y. C. Chen, C. C. Hsieh, C. H. Lin, C. Y. Su, C. K. Yen, Z. H. Liu, W. C. Wang, *Sensor Actuat. A - Phys.*, **216**, 318 (2014)
- [9] H. Yamauchi, M. Sakai, S. Kuniyoshi, K. Kudo, *Jpn. J. Appl. Phys.*, **53**, 01AB16 (2014)
- [10] N.-F. Hsu, M. Chang, K.-T. Hsu, *Mater. Sci. Semicond. Process.*, **21**, 200 (2014)
- [11] D. Panda, T.-Y. Tseng, *J. Mater. Sci.*, **48**, 6849 (2013)
- [12] S. K. Arya, S. Saha, J. E. Ramirez-Vick, V. Gupta, S. Bhansali, S. P. Singh, *Anal. Chim. Acta*, **737**, 1 (2012)
- [13] A. K. Singh, *Adv. Powder Technol.*, **21**, 609 (2010)
- [14] L. Cao, M. K. Li, M. Lu, W. Zhang, Q. Wei, Z. B. Liu, *Mater. Sci. Semicond. Process.*, **11**, 25 (2008)
- [15] N. Preda, M. Enculescu, C. Florica, A. Costas, A. Evangelidis, E. Matei, I. Enculescu, *Dig. J. Nanomater. Biostruct.*, **8**, 1591 (2013)
- [16] S. Xu, Z. L. Wang, *Nano Res.*, **4**, 1013 (2011)
- [17] N. Preda, M. Enculescu, I. Zgura, M. Socol, C. Florica, A. Evangelidis, E. Matei, I. Enculescu, *Zinc Oxide and Polysaccharides: Promising Candidates for Functional Nanomaterials in Size Effects in Nanostructures – Basics and Applications* (V. Kuncser and L. Miu editor), Springer – Verlag, Berlin Heidelberg, 2014.
- [18] M. Gao, J. Liu, H. Sun, X. Wu, D. Xue, *J. Alloys Compd.*, **500**, 181 (2010)
- [19] Q. Tian, J. Li, Q. Xie, Q. Wang, *Mater. Chem. Phys.*, **132**, 652 (2012)
- [20] A. B. Djuricic, A. M. C. Ng, X. Y. Chen, *Progress Quant. Electron.*, **34**, 191 (2010)
- [21] H. Zhou, H. Alves, D.M. Hofmann, W. Kriegseis, B.K. Meyer, G. Kaczmarczyk, A. Hoffmann, *Appl. Phys. Lett.*, **80**, 210 (2002)
- [22] M. Z. Yang, C. L. Dai, C. C. Wu, *Sensors*, **11**, 11112 (2011)
- [23] W. K. Hong, B. J. Kim, T. W. Kim, G. Jo, S. Song, S. S. Kwon, A. Yoon, E. A. Stach, T. Lee, *Colloid Surf. A-Physicochem. Eng. Asp.*, **313-314**, 378 (2008)
- [24] J. Watson, *Sens. Actuator B-Chem.*, **5**, 29 (1984)
- [25] H. Nanto, T. Minami, S. Takata, *J. Appl. Phys.*, **60**, 482 (1986)
- [26] S. Song, W.-K. Hong, S.-S. Kwon, T. Lee, *Appl. Phys. Lett.*, **92**, 263109 (2008)